Chemical Engineering Journal 377 (2019) 120346

Contents lists available at ScienceDirect

Chemical Engineering Journal

journal homepage: www.elsevier.com/locate/cej

Heterogeneous benzaldehyde nitration in batch and continuous flow microreactor

Danilo Russo[a,b], Giovanna Tomaiuolo[b], Roberto Andreozzi[a], Stefano Guido[a], Alexei A. Lapkin[b], Ilaria Di Somma[c,*]

[a] Dipartimento di Ingegneria Chimica, dei Materiali e della Produzione Industriale, Università di Napoli "Federico II", Italy
[b] Department of Chemical Engineering and Biotechnology, University of Cambridge, UK
[c] Istituto di Ricerche sulla Combustione (CNR), Napoli, Italy

HIGHLIGHTS

- Benzaldehyde nitration kinetic model was extended under heterogeneous conditions.
- Batch and continuous flow reactor performances were compared.
- Enhancement of mass transfer was observed in continuous flow static mixer.
- Well designed microreactors can approximate kinetic regime behaviour.

GRAPHICAL ABSTRACT

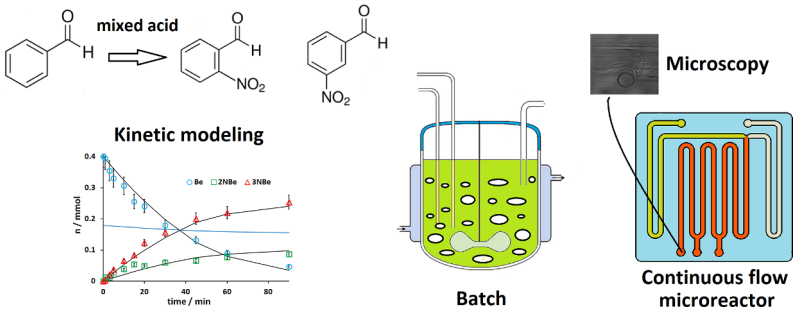

ARTICLE INFO

Keywords:
Nitration
Mixed acid
Benzaldehyde
Heterogeneous
Microreactor
Immiscible liquids

ABSTRACT

Ortho- and meta-nitrobenzaldehydes are two important intermediates in the chemical industry. They are the main products of benzaldehyde nitration by mixed acid, which is a hazardous chemical process since reaction rates are very sensitive to variations of the operating conditions. In the present investigation, a previously developed kinetic model under homogeneous conditions is validated and extended for heterogeneous liquid-liquid systems. A comparison between performances of a lab-scale batch reactor and a commercial microreactor is also presented. The results show that microreactors with embedded static mixer can outperform scaled-up batch reactors, achieving the theoretical limit of conversion/yield attainable under kinetic control.

1. Introduction

Nitrobenzaldehydes are important intermediates involved in the synthesis of many fine chemicals products. Thus, 3-nitrobenzaldehyde is used in the production of pharmaceuticals, plastic additives, frangrances, flavourings, dyes and sector-specific products for galvanometry and X-ray contrast media [1]. The possibility of synthesizing important intermediates for Nicardipine and Pranidipine production has been recently highlighted [2]. Important products synthesised starting from m-nitrobenzaldehyde are 3-hydroxybenzaldeide, 3-nitrobenzoic acid, and rosoxacin, an antigonorrheal agent [3]. 2-Nitrobenzaldehyde is involved in pharmaceutical and dyes industries, and is also used as a photo-removable protecting group for several functional groups, as well as in the synthesis of non-linear optical materials [1,4–8]. Important industrial intermediated prepared starting from o-nitrobenzaldehyde are 2-aminobenzaldehyde, 4-4′-dicholoindingo, and

* Corresponding author.
E-mail address: i.disomma@irc.cnr.it (I. Di Somma).

https://doi.org/10.1016/j.cej.2018.11.044

Available online 08 November 2018
1385-8947/

2H-indazole derivatives [3]. Both isomers are also involved in the preparation of benzodiazepines and other cardiovascular drugs [1]. Nitrobenzaldehydes are both products of nitration of benzaldehyde by means of concentrated mixture of nitric acid, sulfuric acid and water, also called 'mixed acid'. This reaction is among the most hazardous industrial processes [9,10]. It meets all the requirements for the onset of a thermal explosion: (i) high exothermicity, with a heat of reaction ranging from -73 to $-253\,kJ{\cdot}mol^{-1}$ [11], (ii) reaction rate being very sensitive to small variations in the acid mixture composition and operating temperature, and (iii) several secondary exothermic reactions can be triggered as a result of a deviation from the design operating conditions. Traditional benzaldehyde nitration under heterogeneous conditions is carried out in batch or fed-batch reactors, slowly adding the nitrating agent to the organic substrate or vice versa. To prevent the runaway of the system, the process is usually carried out at temperature between $-5\,^{\circ}C$ and $15\,^{\circ}C$ and reaction times up to 6 h, which is economically inconvenient and makes it impossible to control the yield of the two isomers [1,3]. Ideally, for such systems, experimental investigations should be devoted to a complete thermo-kinetic characterization both, under normal operating conditions and as a result of a deviation from the optimum design conditions. In this regard, several works were published about by-products identification [12], dynamic processes evolution [13], kinetics characterization [14,15], thermal decomposition, and calorimetric investigations [16–20]. Following this rationale, in a previous paper a kinetic model was developed to predict benzaldehyde nitration in mixed acid under homogeneous conditions, that is using an organic concentration lower than its solubility. This allowed to estimate intrinsic kinetic parameters, preventing them from being affected by mass transfer limitations. The model was successfully used to investigate benzaldehyde nitration in a commercial microreactor [21]. In fact, for all the above-mentioned reasons, microreactor technology naturally suits the nitration processes management requirements, especially for highly priced and low-throughput materials production or niche technology applications.

However, most nitration processes in mixed acid are carried out in heterogeneous liquid-liquid systems. In fact, organic substrates, as well as reaction products, are often poorly soluble in the aqueous acidic phase where the reaction occurs. The resulting higher complexity of the process requires simultaneous analysis of multiple process hierarchy levels, according to the theoretical framework proposed by Lapkin et al. [22]. Therefore, a first investigation to safely carry out the reaction at higher temperature was reported in the literature by Kulkarni et al. [1]. In this study the experiments were carried out both in batch and continuous mode at temperature, nitric acid to benzaldehyde molar ratio and nitric acid to sulfuric acid molar ration varying in the ranges 5–25 °C, 1.18–3.5, and 0.3–0.6, respectively. Under these conditions, the reactive system is always in immiscible liquid-liquid heterogeneous conditions. The two important aspects highlighted in this study are (i) the need of a good mixing between the two immiscible phase and (ii) the increase in the ratio of the ortho- to the meta-isomer at higher temperature and nitric to sulfuric acid ratios.

Accordingly, in the first part of this work, an extension and validation of the previous model for heterogeneous systems is presented. The experimental validation was carried out in a lab-scale batch reactor under kinetic regime. The developed model provided important information about products partition and the maximum obtainable conversion in the absence of mass transfer limitations.

In the second part, the performance of a microreactor with embedded static mixer (passive mixing techniques) at different conditions was compared. In fact, it has been recently highlighted [14] that microreactor technology importance has been soon acknowledged by the industry both as a useful tool for pilot plant investigations and as a productive unit for specific applications. Microreactors are typically characterized by enhanced heat and mass transfer, which enable precise control of temperature, a great variety of internal structures due to flexibility of modern manufacturing methods, but a relatively low productivity [23]. For these reasons, this technology naturally suits the requirements of nitration processes, especially for manufacture of expensive and low-volume materials. As a result, most nitrations reported in the literature were carried out in microreactors with diameters ranging from hundreds of micrometers to a few millimiters, the latter combining the advantages of micro-scale reactor with higher productivities. As a result, several examples of nitration in microreactors can be found in the literature [1,11,21,24–30]. However, typical lab-scale setups consist of of preheating channels connected to separate pumps to feed organics and nitrating mixtures to a mixing device [25–27,31]. Innovative devices have embedded mixers and heat exchanger to reduce the experimental complexity and achieve higher compactness. Most of the reported processes are carried out in capillary microreactors, under heterogeneous liquid-liquid conditions, with the formation of slugs of organic and acidic aqueous phase. As a general result, increasing the flow rate, an enhancement of mass transfer between the slugs is reported, which is corroborated by CFD calculations [24]. However, meso-scale continuous flow microreactors, as the one adopted in the present investigation, are still poorly investigated, despite the promising results in terms of enhanced productivity. Even though the flow pattern of immiscible liquids in micro-channels has been widely investigated, the results are often reported for simple geometries of the open micro-channel [24,32,33], whereas only a few studies were reported for complex static mixers structures in the reactor [34]. In microchannels with constant internal section, different flow patterns were observed as a result of the competition between shear forces and surface tension. They can be summarized as threading, jetting, dripping, tubing and displacement [35] and they can be related to the capillary dimensionless number, which is related to the ratio between viscous forces and interfacial tension. In the case of passive embedded mixing, the channel of the reactor is internally shaped to continuously mix the phases in order to enhance mass transfer and, as a result, increase the observed reaction rate using a ribbon like structure with contractions, expansions, and obstacles. In this work, we investigate for the first time benzaldehyde nitration in such a commercially available and scaled-up compact system highlighting the possibility to achieve outstanding performances, close the ones under kinetic regime, without the adoption of active micro-mixer devices and starting from relatively low flow rates. The observations were supported by the kinetic model validated in the first part of the work.

2. Materials and methods

2.1. Materials

All reagents (acetonitrile ≥ 99.9%; methanol ≥ 99.9%; phosphoric acid 85 wt% in H2O; benzaldehyde ≥ 99%; 2-nitrobenzaldehyde 98%; 3-nitrobenzaldehyde 99%; 4-nitrobenzaldehyde 98%; benzoic acid ≥ 99.5%; 2-nitrobenzoic acid 95%; 3-nitrobenzoic acid 99%; 4-nitrobenzoic acid 98%; nitric acid fuming ≥ 99%; sulfuric acid 99.999%; urea 99%) were purchased by Sigma-Aldrich and used as received. Bi-distilled water was used to prepare mixed acid solutions.

2.2. Procedures

Experiments were carried out in a glass jacketed reactor (cooling fluid: water) of 10 mL connected to a Julabo F32 refrigerated/heated circulator. The reactor was magnetically stirred (1100 rpm) and equipped with a thermocouple to guarantee isothermal conditions. Proper relative amounts of nitric acid, sulfuric acid, and water were weighted and mixed under continuous cooling in an ice bath and then added in the reactor and heated at the desired temperature. A proper amount of benzaldehyde was then added. At each experimental time, the whole content of the reactor was quenched by dilution (1:10) with a cold solution of urea in acetonitrile ($4\,g{\cdot}L^{-1}$) in which both phases are highly soluble. The samples were further diluted (1:100) in acetonitrile

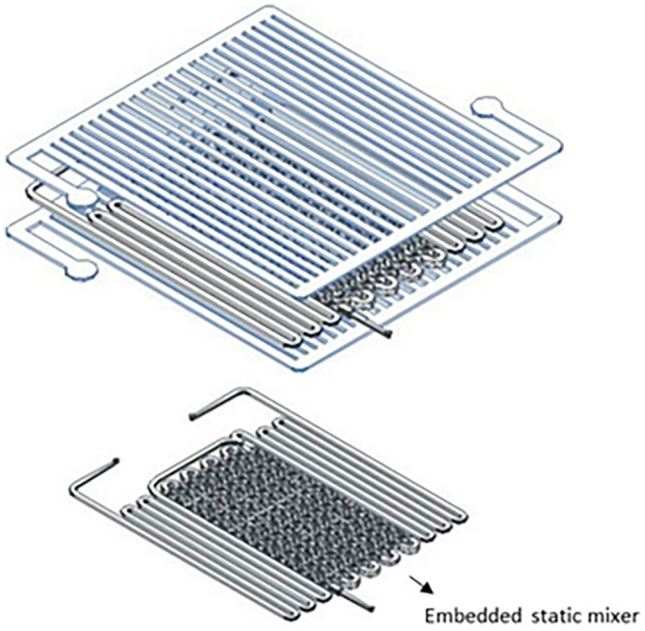

Fig. 1. Exploded view of the adopted commercial microreactor and its embedded static mixer.

and analyzed by HPLC. It was experimentally impossible to sample the two phases separately.

Continuous flow experiments were carried out in a commercially available microreactor (Little Things Factory XXL-ST-04) with embedded static mixer. The experimental setup was already described elsewhere [21], and a scheme of the reactor is reproduced for convenience in the Supporting Information. Specifically, the microreactor channel is internally shaped to continuously mix the phases. In other words, the embedded static mixer consists of a holding line embedded in the reactor to create local turbulence and mixing along the length of the channel. The internal cross-section of the reactor is square (l = 2.2 mm), partially occupied by the mixer holding line (V = 8.0 mL, L = 3.0 m), Fig. 1.

Reagents were separately fed by means of syringe pumps, samples were collected at the outlet of the reactor, quenched and diluted as previously described and analyzed by HPLC. Each experimental run was carried out in triplicate.

To collect microscopy images, a glass Micronit microchip (1000 × 50 μm) was connected to the outlet of the microreactor and placed under an inverted, transmittion light microscop (Axio 100, Zeiss), equipped with a high-speed video camera (Phantom 4.3, capable to record up to 10,000 frames·s^{-1}) and a low magnification objective (10×) was used. The recorded images (600–800 frames·s^{-1}) were analyzed off-line by a commercial software (Image Pro Plus 6.0). The adoption of a glass Micronit chip was necessary to collect in-line images at the outlet port of the reactor since the dimensions of the reactor itself did not allow to place it under the microscope objective (Supplementary Information SI).

To evaluate solubility of organics in mixed acid in the neighborhood of the adopted conditions, poorly reactive or non-reactive acidic solutions were chosen in the neighborhood of the mixed acid compositions adopted for this work. The adoption of poorly reactive solutions was needed to evaluate the solubility of the organics preventing the experimental measurements to be affected by the occurring reactions. Organics were added to the solutions at higher concentrations than their solubility and vigorously mixed for two hours in the batch reactor. Mixing was then stopped for one hour, phases were separated and the acidic aqueous phase was collected, diluted with acetonitrile and analyzed by HPLC. When using solid substrates (2- and 3-nitrobenzaldehyde), the collected samples of the acidic aqueous phase were rapidly filtered using acid resistant filters.

2.3. Analytical methods

Collected samples were analyzed by HPLC Agilent 1100, equipped with a Phenomenex Synergi polar RP/80A column thermostated at 30 °C, and a UV DAD detector. The mobile phase (1.0 mL·min^{-1}) was constituted of eluent (A) (buffer solution: CH_3OH 5% v/v; H_3PO_4 0.4% v/v; H_2O 94.6% v/v) and eluent (B) (acetonitrile). The gradient was as follows: 15% B for 8 min, increased to 25% B in 10 min, and successively decreased to 15% B in 5 min. The signals were acquired at wavelength of 230, 250, and 265 nm.

3. Results and discussion

3.1. Model extension and validation

The result of a standard batch experiment is shown in Fig. 2 together with a concentration profile under homogeneous conditions. As a general result, in the neighbourhood of the standard mixed acid composition (20% wt. HNO_3, 60% wt. H_2SO_4, 20% wt. H_2O), which is normally employed for nitrations in the industry, the only observed nitration products are 2- and 3-nitrobenzaldehyde. 4-Nitrobenzaldehyde, together with the oxidized by products, were not detected or detected only at trace levels. This is in agreement with the previously published data for the homogeneous systems [36–38].

As previously mentioned in Section 2.2, under heterogeneous

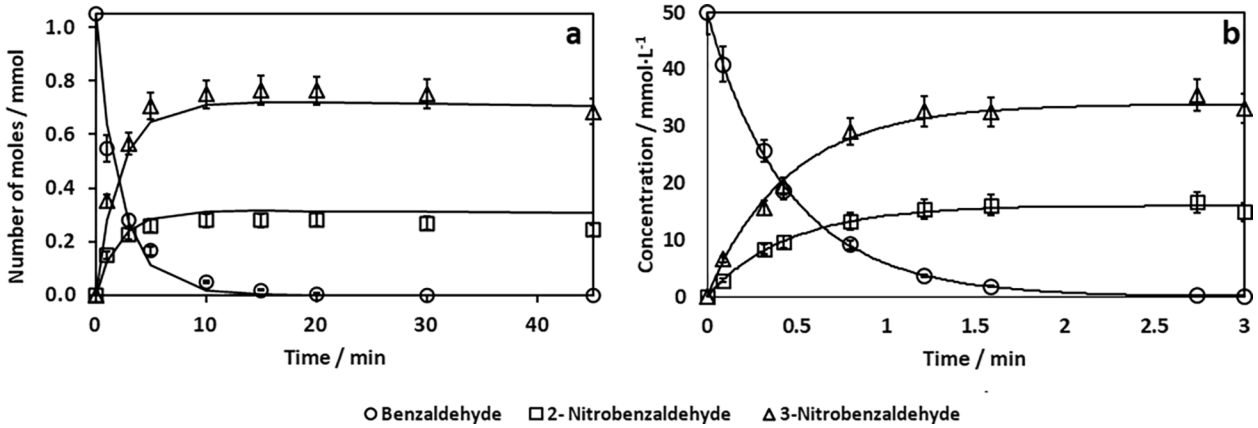

Fig. 2. Experimental batch nitration of benzaldehyde under (a) heterogeneous conditions $V_{org}/V_{mixed\ acid}$ = 0.136; (b) homogeneous conditions C_0 = 50 mmol·L^{-1}. $[HNO_3]_0$ = 5.01 mol·L^{-1}; $[H_2SO_4]_0$ = 10.43 mol·L^{-1}. T = 35 °C.

conditions it was impossible to separately analyse the aqueous and organic immiscible phases. As a result, the total number of moles of each organic in the reactor is the only available experimental result (total volume in the reactor = 1 mL), whereas the actual concentration is reported in the case of homogeneous conditions. As expected, as a first qualitative result, the reaction time to convert a higher amount of benzaldehyde increased significantly, under the same operating conditions, i.e. temperature and acids concentrations. The previously developed kinetic model [38] consisted of a set of differential equations; the formation or consume rate of each organic compound can be calculated according to Eqs. (1) and (2)

$$\frac{dc_i}{dt} = \sum_i r_{N,i} \tag{1}$$

$$r_{N,i} = k^0_{N,i} exp\left(-\frac{E_{aN,i}}{RT}\right)[NO_2^+][Ar_i] \tag{2}$$

where $r_{N,i}$ is the i-th nitration rate in the previously reported reaction mechanism, c_i is the concentration of the species i, $k^0_{N,i}$ and $E_{aN,i}$ the pre-esponential factor and the activation energy, respectively, $[Ar_i]$ the concentration of the aromatic species i, and $[NO_2^+]$ the concentration of nitronium ion in the nitrating mixture. Nitronium ion concentration was evaluated in agreement with the previously reported empirical and semi-empirical equations [38,39]. Its concentration is the equilibrium concentration and it is a known function of the acidic aqueous phase composition. Under homogeneous conditions, the concentration of the aromatics is negligible with respect to the one of nitric acid. As a result the changes in the acid phase composition during the reaction are not significant and the reaction profile is pseudo-first-order-like. On the contrary, under heterogeneous conditions, $[NO_2^+]$ in Eq (2) changes as nitric acid is consumed, and no pseudo-first order kinetic law could fit the data.

The previously developed kinetic model was modified assuming kinetic control of the reaction rate under heterogeneous conditions. The assumption was experimentally verified by comparing the rate of consumption of benzaldehyde and formation of nitrobenzaldehydes at varying stirrer rates. Under the normally adopted conditions for nitration in the lab-scale batch reactor, the experimentally observed reaction rates reached a plateau for magnetic stirrer rates higher than 700 rpm (data not shown). Under these conditions there are no mass transfer limitations and organics are rapidly dissolved in the nitrating mixture up to their solubility thermodynamic limit.

For this reason, batch experiments were carried out at 1100 rpm to guarantee the kinetic control of the reaction and to avoid the introduction of new adjustable parameters in the model. The previously published reaction rates of nitration were modified according to Eqs. (3) and (4) to take into account the actual concentration of organics in the acidic phase.

$$\frac{dn_i}{dt} = \sum_i r^*_{N,i} \tag{3}$$

$$r^*_{N,i} = k^0_{N,i} exp\left(-\frac{E_{aN,i}}{RT}\right)[NO_2^+][Ar_i]^{aq} V^{aq} = k^0_{N,i} exp\left(-\frac{E_{aN,i}}{RT}\right)[NO_2^+] n^{aq}_{Ar,i} \tag{4}$$

where $[Ar_i]^{aq}$ is the concentration of the aromatic species i in the aqueous acidic phase and V^{aq} is the volume of the aqueous acidic phase. Eqs. (3) and (4) take into account the overall number of moles n_i consumed which is controlled by reaction kinetics in the acidic phase, where the reactions occur. The volume of the aqueous acidic phase and the solubility of organics changed during the reaction as nitric acid is consumed, whereas water is formed. In fact, in this case, for each mole of nitrated organic substrate one mole of nitric acid is consumed and one mole of water is formed according to the previously published reaction mechanism [38]. As a result $[NO_2^+]$ varies during time. Moreover, dissolved organics can contribute to variations in the volume of the acidic mixture. Even though in most cases the organic concentration in the acidic phase was negligible with respect to the total molar concentration of water and acids, the additive volumes simplifying hypothesis was adopted for dissolved benzaldehyde, together with dissolved nitrobenzaldehydes according to Eq. (5).

$$V^{aq}(t) = V^{mix}(t) + V^{Ar}_{diss}(t) \tag{5}$$

$$V^{Ar}_{diss}(t) = \sum_i \frac{n^{aq}_{Ar,i} MW_i}{\rho_i} \tag{6}$$

where V^{mix} is the volume of the nitrating mixture, V^{Ar}_{diss} the volume of the dissolved organics, $V^{aq}(t)$ the total volume of the aqueous acidic phase, and MW_i and ρ_i the molar weight and density of the i-th species, respectively.

In Eq. (6), $n^{aq}_{Ar,i}$ are equal to the maximum dissolved moles of the organic species i, according to its solubility in the mixture, as long as the amount of the organic in the reactor is higher than its solubility, and becomes equal to the total moles of the species i in the system once its amount drops below the solubility value.

Solubility of the organics in mixed acid at varying composition and temperature where separately investigated through independent experiments. Their values were found to be independent of the presence of the other organics in the system at the adopted concentrations. The logarithm of the organic molar fraction was linearly dependent on the reciprocal of the absolute temperature as shown for some experimental runs in Fig. 3. This is in agreement with previous observations about the solubility of organics in concentrated acid mixtures [40].

At a fixed temperature, empirical linear and quadratic correlations were found between the logarithm of the i-th organic species molar fraction and the total molar acid concentration, in the neighborhood of the investigated conditions for reaction kinetics. The empirical expressions can be summarized as follows:

$$\ln X_{Be} = 0.593 \cdot ([HNO_3] + [H_2SO_4]) + 0.0108 \cdot T - 16.771 if\ [HNO_3] + [H_2SO_4] > 12.9 mol \cdot L^{-1} \tag{7}$$

$$\ln X_{2NBe} = 0.030 \cdot ([HNO_3] + [H_2SO_4])^2 + 0.0428 \cdot T - 20.729 \tag{8}$$

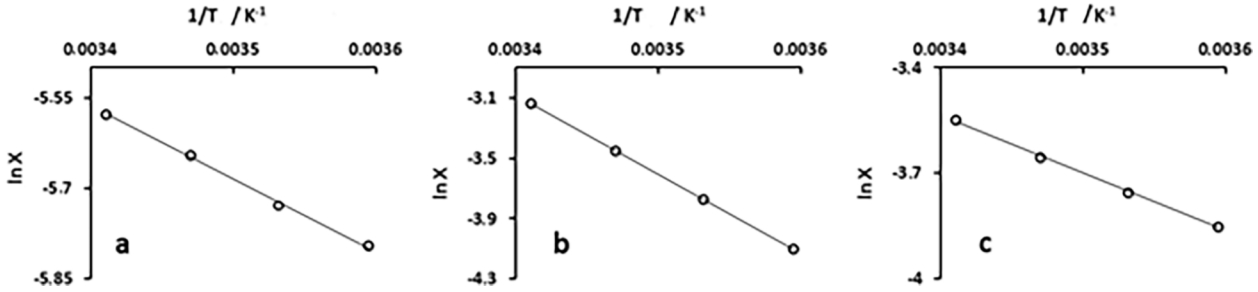

Fig. 3. Solubility dependence on temperature for (a) benzaldehyde, $[HNO_3] = 6.60\ mol \cdot L^{-1}$, $[H_2SO_4] = 6.76\ mol \cdot L^{-1}$; (b) 3-nitrobenzaldehyde, $[HNO_3] = 3.79\ mol \cdot L^{-1}$, $[H_2SO_4] = 11.32\ mol \cdot L^{-1}$; (c) 2-nitrobenzaldehyde, $[HNO_3] = 1.90\ mol \cdot L^{-1}$, $[H_2SO_4] = 10.25\ mol \cdot L^{-1}$.

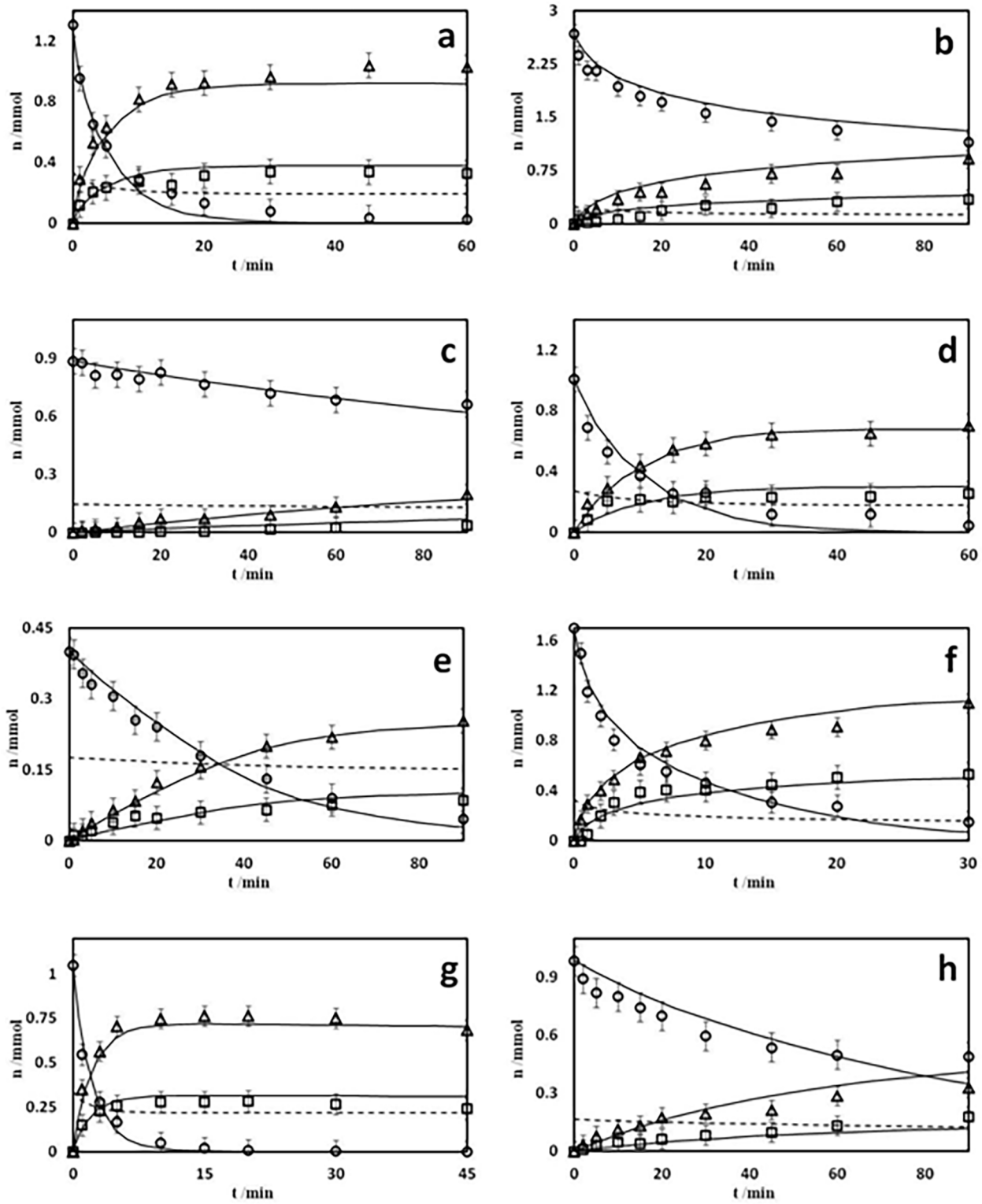

Fig. 4. Comparison between experimental and calculated data. Experimental conditions are summarized in Table 1. (○) benzaldehyde; (□) 2-nitrobenzaldehyde; (Δ) 3-nitrobenzaldehyde.

$$\ln X_{3NBe} = 0.403 \cdot ([HNO_3] + [H_2SO_4]) + 0.0492 \cdot T - 23.961 \quad (9)$$

where X and $[i]$ is the molar fraction and the molar concentration of the species i, respectively, and T the absolute temperature in K. It is worth noting that solubilities of the 2- and 3-nitrobenzaldehydes is 1–2 orders of magnitude higher than that of benzaldehyde. The above Eqs. (3)–(9) were simultaneously solved to predict the molar consumption of benzaldehyde and formation of 2- and 3-nitrobenzaldehydes under heterogeneous liquid-liquid conditions. The calculated and experimental data were compared in Fig. 4 for some of the adopted experimental conditions. As shown, the model was capable of predicting the experimental consumption and formation rates without any further adjustment of the previously estimated intrinsic kinetic parameters [38] (See Table 1).

Table 1
Adopted experimental conditions for the runs presented in Fig. 4.

Run	T/°C	HNO_3 wt%	H_2SO_4 wt%	$V_{org}/V_{mixed\ acid}$
a	15	23.02	62.85	0.167
b	15	22.73	62.05	0.333
c	25	20.13	58.52	0.099
d	25	23.26	59.74	0.122
e	25	20.85	58.52	0.047
f	25	22.36	63.21	0.205
g	35	20.97	63.61	0.136
h	35	20.37	58.43	0.111

3.2. Enhancement of mass transfer in microreactor with embedded static mixer

According to Taminu et al. [41], for two immiscible phases the most common flow patterns are parallel flow, segmented flow, annular flow and dispersed flow. It is worth noting that for channels without embedded static mixer, the transition between the different regimes is determined by variations of about one order of magnitude in the flow rate [42].

Preliminary images collected at the outlet of a liquid-liquid microreactor with embedded static mixer are reported in Fig. 5 at different flow rates, but similar reaction times. In Fig. 5, in each row are reported three representative frames at a fixed flow rate. The aim of this preliminary investigation is to show that significantly different flow patterns can be achieved in microreactors as the one adopted in this investigation, even for small changes in the flow rate. The result is relevant if one considers that using tubular reactors at the same flow rates only parallel flow or slugs were observed in the literature depending on the internal diameter of the channels [11,43,44].

As shown, a threading stable flow pattern is observed, under the adopted conditions, at a flow rate of 20 $\mu L \cdot min^{-1}$ with a liquid core formation of the organic phase surrounded by the aqueous acidic phase, Fig. 5a. Increasing the flow rate, the organic thread becomes thinner with the occasional formation of big organic droplets with diameters comparable with the internal diameter of the channel, Fig. 5b. The thread thinning is enhanced at higher flow rates with the first occasional instability of the organic thread observed at 60 $\mu L \cdot min^{-1}$, under the adopted conditions, Fig. 5c. The instability is associated with the formation of a large number of smaller droplets. An increasingly marked instability effects is observed at 80 $\mu L \cdot min^{-1}$ with the occasional reformation of an unstable organic thread. Two unstable threads are finally observed at 100 $\mu L \cdot min^{-1}$.

As already reported, as a general qualitative result, the mass transfer between the phases is enhanced at higher flow rates. However, it must be noted that, as a result of the presence of an embedded static mixer, small increments in the flow rate can result in completely different flow patterns with a higher predicted conversion.

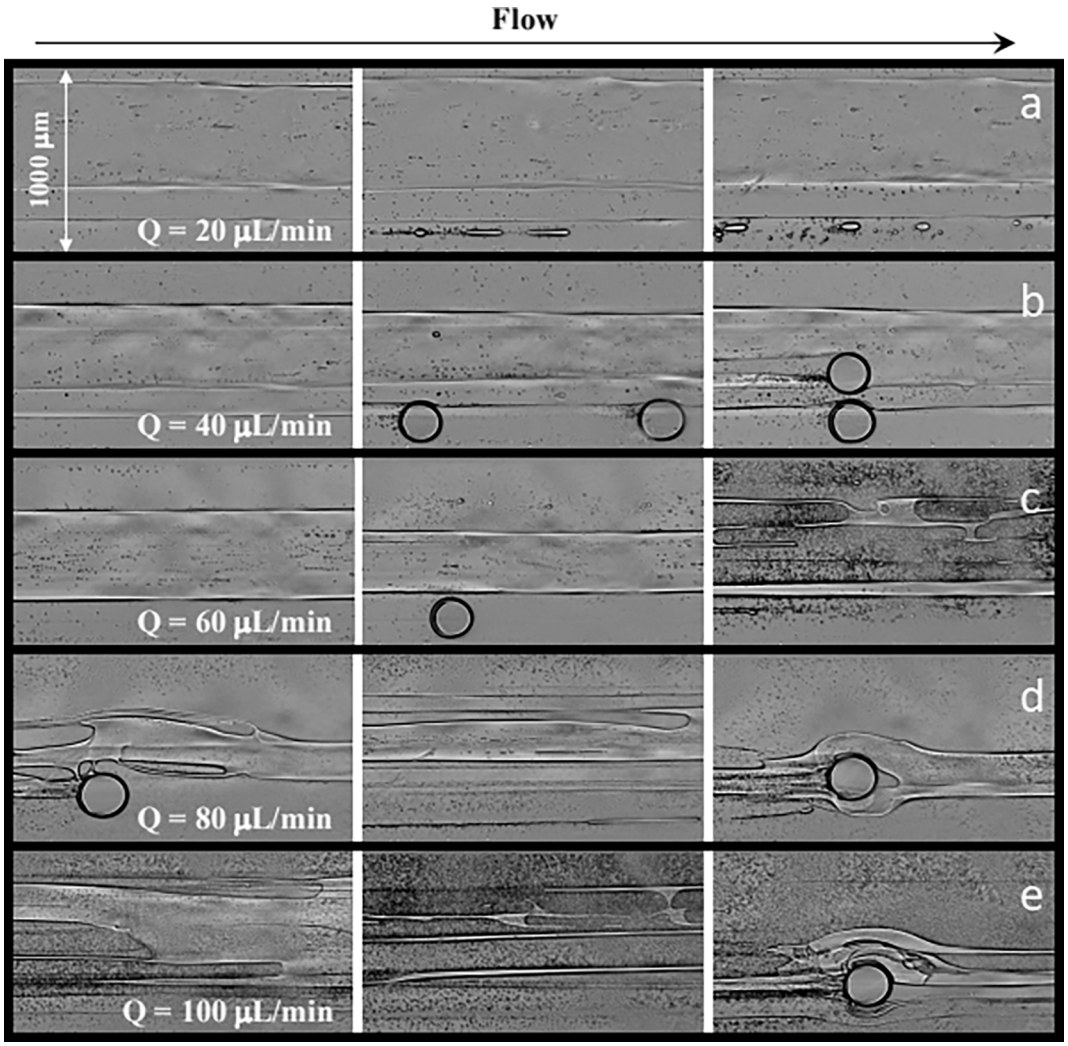

Fig. 5. Flow patterns at different flow rates at the outlet of the static mixer of the microreactor. T = 20 °C; 20% wt. HNO_3, 60% wt. H_2SO_4. Q = $Q_{organic}$ = $Q_{mixed\ acid}$. In each row are shown significant frames at the reported flow rate. Channel dimension = 1000 µm.

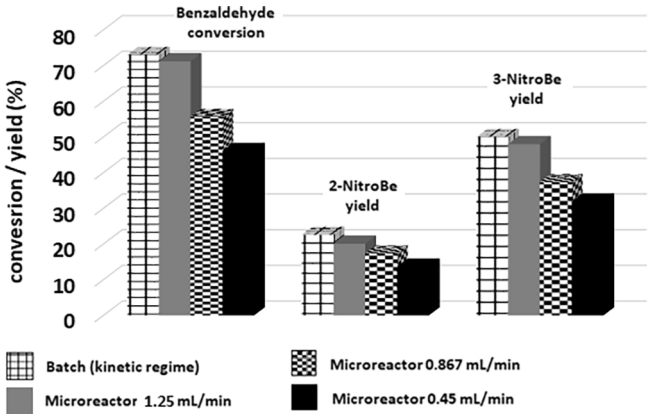

Fig. 6. The comparison between the performances of small-scale batch reactor and microreactor with embedded static mixer at different flow rates. T = 35 °C; $[HNO_3] = 5.0\ mol{\cdot}L^{-1}$, $[H_2SO_4] = 10.4\ mol{\cdot}L^{-1}$; $\tau = 3.6$ min.

3.3. Lab-scale batch reactor vs. microreactor with embedded static mixer

The qualitative preliminary results presented in Section 3.2 were confirmed by the analytical results. In all the previously reported nitrations in microreactos [11], although the observed reaction rate was found to increase in microreactors, there is no direct proof that the adopted devices are working under kinetic control. A few more detailed studies [43,44] carried out using simple tubular section reactors, quasi-kinetic regime is suggested to be achieved at LHSV values higher than $2000\ h^{-1}$, corresponding to very low residence times and, hence, to relatively high values of flow rates. A comparison between performances of a lab-scale batch reactor and a continuous flow microreactor with embedded static mixer at varying flow-rate is reported in Fig. 6, in terms of benzaldehyde conversion and nitrobenzaldehydes yields at a fixed reaction time/residence time (τ).

There was no significant difference in the products partition under all the investigated conditions, which suggests a good mixing within each of the phases. However, a significantly different benzaldehyde conversion was observed. As expected, higher conversion is achieved at higher flow rates, even though always lower than in a lab-scale batch reactor under kinetic regime. Performances very similar to those attained under kinetic control of the reaction were achieved at a flow rate of 1.25 mL/min. It must be noted that in the scaled-up batch reactors, mixing conditions that allow to reach kinetic control of a reaction are very unlikely and, in most cases, impossible to be achieved. Therefore, the results suggest that well-designed microreactors with embedded static mixers can achieve targets similar to those achieved under kinetic regime, which is a further process intensification in combination with the previously reported benefits in terms of yield and selectivity [21] and the advantage of using meso-scale reactors, which provide high productivity. It must be stressed that the significant enhancement of mass transfer between the phases allows to attain the theoretical limit of conversion/yield at the shortest residence time. In order to prove this point, experimental runs were carried out using higher flow rates up to $10\ mL{\cdot}min^{-1}$, and the results were compared with those predicted by the batch model for the same reaction time. Harsher conditions, that are highly acidic media, were used to carry out experiments at higher flow rates to achieve high conversion at short residence times. As an example, an experimental benzaldehyde conversion of 97% was achieved in the microreactor adopting the following conditions: $Q_{tot} = 9.22\ mL{\cdot}min^{-1}$, $Q_{mixed\ acid}/Q_{organic} = 4.94$, T = 25 °C, $[HNO_3] = 6.03\ mol{\cdot}L^{-1}$, $[H_2SO_4] = 12.09\ mol{\cdot}L^{-1}$. In the same conditions, benzaldehyde conversion of 99% was predicted by the model for the batch reactor under kinetic regime.

Therefore, the kinetic model developed in Section 3.1 can be a useful tool to predict products partition and maximum achievable conversion in well-designed microreactor devices.

4. Conclusions

In the present investigation, a previously developed kinetic model for benzaldehyde nitration under homogeneous conditions was extended and validated under heterogeneous conditions. The model prediction were in agreement with experimental results, without any further adjustment of the previously estimated kinetic parameters. The same liquid-liquid heterogeneous reaction was carried out in a commercially available microreactor with embedded static mixer. The results showed that microreactors with embedded static mixer are promising alternatives to scaled-up batch reactors to carry out nitrations and can achieve kinetic regime at relatively low flow-rates. The conclusions were supported by preliminary microscopic observations, which demonstrated a significant change in the flow pattern for small variations in the adopted flow rate in such designed systems. Further investigation will be devoted to identify and map different regimes at varying experimental conditions.

Appendix A. Supplementary data

Supplementary data to this article can be found online at https://doi.org/10.1016/j.cej.2018.11.044.

References

[1] A.A. Kulkarni, V.S. Kalyani, R.A. Joshi, R.R. Joshi, Continuous flow nitration of benzaldehyde, Org. Process Res. Dev. 13 (2009) 999–1002.
[2] K. Neelakandan, H. Manikandan, B. Prabhakaran, N. Santosha, A. Chaudhari, M. Kulkarni, G. Mannathusamy, S. Titirmare, Synthesis, isolation and use of a common key intermediate for calcium antagonist inhibitors, Der Pharm. Sin. 5 (2014) 11–17.
[3] F. Bruhne, Nitro Compounds, aromatic, Ullmann's Encyclopedia of Industrial Chemistry, Wiley-VCH, 2003.
[4] Y. Wang, W. Tam, S.H. Stevenson, R.A. Clement, J. Calabrese, New organic non-linear optical materials of stilbene and diphenylacetylene derivatives, Chem. Phys. Lett. 148 (1988) 136–141.
[5] P. Sebej, T. Solomek, L. Hroudnà, P. Brancovà, P. Klàn, Photochemistry of 2-nitrobenzylidene acetals, J. Org. Chem. 74 (2009) 8647–8658.
[6] S.A. Abubshait, R.R. Kassab, A.H. Al-Shehri, H.A. Abubshait, Synthesis and reactions of some novel 4-biphenyl-4-(2H)-phthalazin-1-one derivatives with an expected antimicrobial activity, J. Saudi Chem. Soc. 15 (2011) 59–65.
[7] E.A. Chigorina, 1-cyanoacetyl-3,5-dimethylpyrazole, Synlett 25 (2014) 453–454.
[8] A.R. Maddirala, P.R. Andreana, Synthesis of 3-substituted 2-indolinones by a multicomponent coupling isocyanide-dependent microwave-assisted intramolecular transamidation process, Eur. J. Org. Chem. 196–209 (2016).
[9] J.A. Barton, P.F. Nolan, Incidents in the chemical industry due to thermal-runaway chemical reactions, IChemE Sympos. Ser. 115 (1989) 3–17.
[10] R. Saada, D. Patel, B. Saha, Causes and consequences of thermal runaway incidents – will they ever be avoided? Process Saf. Environ. Prot. 97 (2015) 109–115.
[11] A.A. Kulkarni, Continuous flow nitration in miniaturized devices, Beilstein J. Org. Chem. 10 (2014) 405–424.
[12] A. Lunghi, M.A. Alos, L. Gigante, J. Feixas, E. Sironi, J.A. Feliu, P. Cardillo, Identification of the decomposition products in an industrial nitration process under thermal runaway conditions, Org. Process Res. Dev. 6 (6) (2002) 926–932.
[13] R. Ball, B.F. Gray, Thermal instability and runaway criteria: the dangers of disregarding dynamics, Process Saf. Environ. Prot. 91 (2013) 221–226.
[14] R. Andreozzi, M. Canterino, V. Caprio, I. Di Somma, R. Sanchirico, Salicylic acid nitration by means of nitric acid/acetic acid system: chemical and kinetic characterization, Org. Process Res. Dev. 10 (6) (2006) 1199–1204.
[15] I. Di Somma, R. Marotta, R. Andreozzi, V. Caprio, Kinetic and safety characterization of the nitration process of methyl benzoate in mixed acid, Org. Process Res. Dev. 16 (12) (2012) 2001–2007.
[16] K.R. Westerterp, E.J. Molga, Safety and runaway prevention in batch and semibatch reactors – a review, Chem. Eng. Res. Des. 84 (7) (2006) 543–552.
[17] L.P. Chen, T.T. Liu, Q. Yang, W.H. Chen, Thermal hazard evaluation for iso-octanol nitration with mixed acid, J. Loss Prev. Process Ind. 25 (2012) 631–635.
[18] J.L. Gustin, Thermal stability screening and reaction calorimetry. Application to runaway reaction hazard assessment and process safety management, J. Loss Prev. Process Ind. 6 (5) (1993) 257–291.
[19] B. Das, P. Mondal, S. Kumar, Pressurization studies in a sealed autoclave for thermal decomposition of nitrated TBP and TiAP, J. Radional. Nucl. Chem. 288 (2011) 641–643.
[20] L.K. Patil, V.G. Gaikar, S. Kumar, U.K. Mudali, R. Natarajan, Thermal decomposition of nitrated tri-n-butyl phosphate in a flow reactor, ISRN Chem. Eng. (2012) 1–9.

[21] D. Russo, I. Di Somma, R. Marotta, G. Tomaiuolo, R. Andreozzi, S. Guido, A.A. Lapkin, Intensification of nitrobenzaldehydes synthesis from benzyl alcohol in a microreactor, Org. Process Res. Dev. 21 (3) (2017) 357–364.
[22] A.A. Lapkin, A. Voutchkova, P. Anastas, A conceptual framework for description of complexity in intensive chemical processes, Chem. Eng. Process. 50 (2011) 1027–1034.
[23] A. Lapkin, P.K. Plucinski, Engineering factors for efficient flow processes in chemical industries, in: S.V. Luis, E. Garcia-Verdugo (Eds.), Chemical Reactions and Processes under Flow Conditions, RSC, Cambridge, 2010, pp. 1–43.
[24] G. Dummann, U. Quittmann, L. Groschel, D.W. Agar, O. Worz, K. Morgenschweis, The capillary-microreactor: a new reactor concept for the intensification of heat and mass transfer in liquid-liquid reactions, Catal. Today 79 (2003) 433–439.
[25] R. Halder, A. Lawal, R. Damavarapu, Nitration of toluene in a microreactor, Catal. Today 125 (1–2) (2007) 74–80.
[26] S. Loebbecke, J. Antes, W. Ferstl, D. Boskovic, T. Tuercke, M. Schwarzer, H. Krause, Microreactors for processing of hazardous and explosible reactions, IChemE Sympos. Ser. 153 (2007) 1–6.
[27] J.R. Burns, C. Ramshaw, A microreactor for the nitration of benzene and toluene, Chem. Eng. Commun. 189 (12) (2002) 1611–1628.
[28] C. Zhang, J. Zhang, G. Luo, Kinetic study and intensification of acetyl guaiacol nitration with nitric acid-acetic acid system in a microreactor, J. Flow Chem. 6 (4) (2016) 309–314.
[29] N.B. Zuckerman, M. Shusteff, P.F. Pagoria, A.E. Gash, Microreactor flow synthesis of the secondary high explosive 2,6-diamino-3,5-dinitropyrazine-1-oxide (LLM-105), J. Flow Chem. 5 (3) (2015) 178–182.
[30] L. Li, C. Yao, F. Jiao, M. Han, C. Guangwen, Experimental and kinetic study of the nitration of 2-ethylhexanol in capillary microreactors, Chem. Eng. Process. 117 (2017) 179–185.
[31] A.A. Kulkarni, N.T. Nivangune, V.S. Kalyani, R.A. Joshi, R.R. Joshi, Continuous flow nitration of salicylic acid, Org. Process Res. Dev. 12 (5) (2008) 995–1000.
[32] A.J. Soares, R.L. Thompson, D.C. Niero, Immiscible liquid-liquid pressure-driven flow capillary in tubes: experimental results and numerical comparisons, Phys. Fluids 27 (2015) 1–13.
[33] M.N. Kashid, D.W. Agar, Hydrodynamics of liquid-liquid slug flow capillary microreactor: flow regimes, slug size and pressure drop, Chem. Eng. J. 131 (2007) 1–13.
[34] P. Plouffe, D.M. Roberge, A. Macchi, Liquid-liquid flow regimes and mass transfer in various micro-reactors, Chem. Eng. J. 300 (2016) 9–19.
[35] T. Cubaud, T. Mason, Capillary threads and viscous droplets in square microchannels, Phys. Fluids 20 (5) (2008) 053302.
[36] C.I. Sainz-Diaz, A new approach to the synthesis of 2-nitrobenzaldehyde. Reactivity and molecular structure studies, Monatsh. Chem. 133 (2002) 9–22.
[37] I. Di Somma, R. Marotta, R. Andreozzi, V. Caprio, Increasing yield of 2-nitrobenzaldehyde during benzaldehyde nitration by mixed acid: chemical and safety investigation, Chem. Eng. Trans. 36 (2014) 181–186.
[38] D. Russo, L. Onotri, R. Marotta, R. Andreozzi, I. Di Somma, Benzaldehyde nitration by mixed acid under homogeneous condition: a kinetic modeling, Chem. Eng. J. 307 (2017) 1076–1083.
[39] D. Russo, R. Marotta, M. Commodo, R. Andreozzi, I. Di Somma, Ternary HNO_3-H_2SO_4-H_2O mixture: a simplified approach for the calculation of the equilibrium composition, Ind. Eng. Chem. Res. 57 (5) (2018) 1696–1704.
[40] R. Andreozzi, M. Canterino, V. Caprio, I. Di Somma, R. Sanchirico, Solubility od 5-nitro- and 3-nitrosalicylic acids in an acetic acid/nitric acid mixture, J. Chem. Eng. Data 52 (1) (2007) 122–125.
[41] A. Tanimu, S. Jaenicke, K. Alhooshani, Heterogeneous catalysis in continuous flow microreactors: a review of methods and applications, Chem. Eng. J. 327 (2017) 792–821.
[42] Y. Zhao, G. Chen, Q. Yuan, Liquid-liquid two phase flow patterns in a rectangular microchannel, AIChE J. 52 (12) (2006) 4052–4060.
[43] Z. Yu, Y. Lv, C. Yu, W. Su, A high-output, continuous selective and heterogeneous nitration of p-difluorobenzene, Org. Process Res. Dev. 17 (3) (2013) 438–442.
[44] Y. Chen, Y. Zhao, M. Han, C. Ye, M. Dang, G. Chen, Safe, efficient and selective synthesis of dinitro herbicides via a multifunctional continuous-flow microreactor: one-step dinitration with nitric acid as agent, Green Chem. 15 (2013) 91–94.